Parallel Simulation of Complex Unsteady Flows with Variational Multiscale LES and Hybrid RANS/LES

Hilde Ouvrard, Bruno Koobus, Maria Vittoria Salvetti, Simone Camarri, Stephen Wornom, Alain Dervieux

INSTITUT NATIONAL DE RECHERCHE EN INFORMATIQUE ET EN AUTOMATIQUE

Parallel Simulation of Complex Unsteady Flows with Variational Multiscale LES and Hybrid RANS/LES

H. Ouvrard, B. Koobus, M.-V. Salvetti, S. Camarri, S. Wornom, A. Dervieux

N° 6917

Avril 2009

Thème NUM

ISSN 0249-6399 ISRN INRIA/RR--6917--FR+ENG

Parallel Simulation of Complex Unsteady Flows with Variational Multiscale LES and Hybrid RANS/LES

H. Ouvrard*, B. Koobus†, M.-V. Salvetti‡, S. Camarri§, S. Wornom¶, A. Dervieux‖

Thème NUM — Systèmes numériques
Projet Pumas

Rapport de recherche n° 6917 — Avril 2009 — 17 pages

Abstract: We study a new hybrid RANS/Variational Multiscale LES (VMS-LES) model for bluff body flows. The simulations have been carried out using a parallelized solver, based on a mixed finite element/finite volume formulation on unstructured grids. Parallel performances are analysed. The behavior of a VMS-LES model with different subgrid scale models is investigated for the flow past a circular cylinder at Reynolds number Re =3900. Second, a new strategy for blending RANS and LES methods in a hybrid model is described and applied to the simulation of the flow around a circular cylinder at $Re = 140000$.

Key-words: Bluff-body flows, variational multiscale LES, hybrid RANS/LES approach, parallel simulation

* University of Montpellier II, 34095 Montpellier, France, houvrard@darboux.math.univ-montp2.fr
† University of Montpellier II, 34095 Montpellier, France, koobus@math.univ-montp2.fr
‡ Università di Pisa, Via G. Caruso, 56122 Pisa, Italy, mv.salvetti@ing.unipi.it
§ Università di Pisa, Via G. Caruso, 56122 Pisa, Italy, s.camarri@ing.unipi.it
¶ Lemma, Sophia-Antipolis, France, stephen.wornom@sophia.inria.fr
‖ INRIA, BP. 93, 06902 Sophia-Antipolis, France, alain.dervieux@inria.fr

Unité de recherche INRIA Sophia Antipolis
2004, route des Lucioles, BP 93, 06902 Sophia Antipolis Cedex (France)
Téléphone : +33 4 92 38 77 77 — Télécopie : +33 4 92 38 77 65

Simulation parallèle d'écoulement instationnaires complexes avec VMS-LES et un modèle hybride RANS/LES

Résumé : On étudie un nouveau modéle hybride de turbulence reposant sur RANS et sur des modèles VMS-LES. Les calculs sont réalisés à l'aide d'un algorithme parallèle basé sur une formulation mixte-élément-volume finis sur maillage non-structuré. Les performances sur architecture parallèle sont analysées. Le comportement d'un modèle VMS-LES avec différents modèles sous-grille est étudié pour le cas d'un écoulement autour d'un cylindre à nombre de Reynolds Re =3900. Puis, une nouvelle stratégie de combinaison d'un modèle RANS avec un modèle LES sous forme d'un modèle hybride est décrite et appliquée à la simulation d'un écoulement autour d'un cylindre à un nombre de Reynolds $Re = 140000$.

Mots-clés : Écoulement autour d'un obstacle arrondi, variational multiscale LES, approche hybride RANS/LES, simulation parallèle

1 Introduction

The approach involving the Reynolds-Averaged Navier-Stokes equations (RANS) is widely used for the simulation of complex turbulent flows. However these models are not sufficient to properly simulate complex flows with massive separations such as the flow around bluff bodies. The LES approach gives generally more accurate predictions but requires higher computational cost.

The traditional LES approach is based on a filtering operation, the large energy-containing scales are resolved and the smallest scales are modeled using a sub-grid scale (SGS) model. Usual LES subgrid stress modeling strategies, as for instance the Smagorinsky model, are based on the assumption of an universal behavior of the subgrid scales. Within this assumption, energy-containing eddies should not be filtered. Then large Reynolds numbers cannot be addressed with reasonable coarse meshes, except, in particular regions of detached eddies. Even in the case of low Reynolds number or detached eddies, a particular attention must be paid to energetic eddies. For example, the classical eddy-viscosity models are purely dissipative. Often unable to model backscatter, they apply, instead, damping to large resolved energetic eddies.

Starting from these remarks, we investigate the application of the Variational Multiscale (VMS) concept of Hughes. The VMS approach was originally introduced by Hughes [5, 6] for the LES of incompressible flows and implemented in a Fourier spectral framework using a frequency cutoff for the scale separation (small and large scales). In this approach, the Navier-Stokes equations are not filtered but are treated by variational projection, and the effect of the unresolved scales is modeled only in the equations representing the small resolved scales. The VMS-LES approach (even with simple subgrid scale models as Smagorinsky's model) and dynamic LES models have shown similar order of accuracy, but the former is less computationally expensive and does not require any *ad hoc* treatement (smoothing and clipping of the dynamic constant, as usually required with dynamic LES models) in order to avoid stability problems. In this work, we consider the VMS-LES implementation presented in [10] for the simulation of compressible turbulent flows on unstructured grids within a mixed finite volume/finite element framework. We investigate the effect of subgrid scale models in our VMS-LES method for the simulation of a bluff-body flow.

Another major difficulty for the success of LES for the simulation of complex flows is the fact that the cost of LES increases as the flow Reynolds number is increased. Indeed, the grid has to be fine enough to resolve a significant part of the turbulent scales, and this becomes particularly critical in the near-wall regions. A new class of models has recently been proposed in the literature in which RANS and LES approaches are combined together in order to obtain simulations as accurate as in the LES case but at reasonable computational costs. Among these so-called hybrid models described in the literature, the Detached Eddy Simulation (DES) [24] has received the largest attention. In previous works, we proposed a new strategy for blending RANS and LES approaches in a hybrid model [20, 18]. To this purpose, as in [12], the flow variables are decomposed in a RANS part (i.e. the averaged flow field), a correction part that takes into account the turbulent large-scale fluctuations, and a third part made of the unresolved or SGS fluctuations. The basic idea is to solve the RANS equations in the whole computational domain and to correct the obtained averaged flow field by adding, where the grid is adequately refined, the remaining resolved fluctuations. We search here for a hybridization strategy in which the RANS and LES models are blended in the computational domain following a given criterion. To this aim, a blending function is introduced, θ, which smoothly varies between 0 and 1. In particular, two different definitions of the blending function θ are proposed and examined in this paper. They are based on the ratios between (i) two eddy viscosities and (ii) two characteristic length scales. The RANS model used in the proposed

hybrid approach is a low-Reynolds number version [4] of the standard $k-\varepsilon$ model, while for the LES part the Variational Multiscale approach (VMS) is adopted [5].

In this paper, we present VMS-LES and RANS/VMS-LES parallel simulations of bluff-body flows, by a computational fluid dynamics (CFD) software which combines mesh partitioning techniques and a domain decomposition method. These simulations require the discretization of the fluid equations on large three-dimensional meshes with small time-steps. Therefore they require intensive computational resources (in terms of CPU and memory) and parallel computation is of particular interest for such applications. We shall describe in short our solution algorithm and compare its performance for two different paralle architectures.

2 Turbulence modeling

2.1 Variational Multiscale LES

In this paper, we consider the *Koobus-Farhat VMS implementation* [10] for the simulation of compressible turbulent flows. It uses the flow variable decomposition [5],[3]:

$$W = \underbrace{\overline{W}}_{LRS} + \underbrace{W'}_{SRS} + W^{SGS} \tag{1}$$

where $\overline{W}$ is the large resolved scale (LRS) component of W, W' is its small resolved scale (SRS) component, and W^{SGS} the non-resolved component. The decomposition of the resolved component is obtained by projection onto two complementary spaces $\overline{\mathcal{W}}$ (LRS space) and $\mathcal{W}'$ (SRS space) of the resolved scale space:

$$\overline{W} \in \overline{\mathcal{W}} \quad ; \quad W' \in \mathcal{W}' \ . \tag{2}$$

A projector operator onto the LRS space $\overline{\mathcal{W}}$ is defined by spatial averaging on macro cells, obtained by finite-volume agglomeration which splits the basis/test functions ϕ_l into large scale basis denoted $\overline{\phi}_l$, and small scale basis denoted ϕ'_l.

$$\overline{W} = \sum \overline{W}_l \overline{\phi}_l \quad ; \quad W' = \sum W'_l \phi'_l \tag{3}$$

By variational projection onto $\overline{\mathcal{W}}$ and $\mathcal{W}'$, we obtain the equations governing the large resolved scales and the equations governing the small resolved scales. A key feature of the VMS model is that we set to zero the modeled influence of the unresolved scales on the large resolved ones. The SGS model is introduced only in the equations governing the small resolved scales, and, by combining the small and large resolved scale equations, the resulting Galerkin variational formulation of the VMS model writes:

$$\left(\frac{\partial(\overline{W}+W')}{\partial t}, \phi_l\right) + \left(\nabla \cdot F(\overline{W}+W'), \phi_l\right) = -\left(\ \tau^{LES}(W'), \phi'_l\right) \quad l = 1, N \tag{4}$$

where F reprents both convective and viscous terms and $\tau^{LES}(W')$ is the subgrid scale tensor computed using the SRS component, defined by a SGS eddy-viscosity model.

For the purpose of this study, three SGS eddy-viscosity models are considered: the classical model of Smagorinsky [23], and two recent and promising models, namely the WALE model [16] and the one of Vreman [27]. More details on this VMS-LES approach can be found in [10].

2.2 Hybrid RANS/VMS-LES

As in Labourasse and Sagaut [12], the following decomposition of the flow variables is adopted:

$$W = \underbrace{< W >}_{RANS} + \underbrace{W^c}_{correction} + W^{SGS}$$

where $< W >$ are the RANS flow variables, obtained by applying an averaging operator to the Navier-Stokes equations, W^c are the remaining resolved fluctuations (i.e. $< W > + W^c$ are the flow variables in LES) and W^{SGS} are the unresolved or SGS fluctuations.

If we write the Navier-Stokes equations in the following compact conservative form:

$$\frac{\partial W}{\partial t} + \nabla \cdot F(W) = 0$$

in which F represents both the viscous and the convective fluxes, for the averaged flow $\langle W \rangle$ we get:

$$\frac{\partial \langle W \rangle}{\partial t} + \nabla \cdot F(\langle W \rangle) = -\tau^{RANS}(\langle W \rangle) \tag{5}$$

where $\tau^{RANS}(\langle W \rangle)$ is the closure term given by a RANS turbulence model.

As well known, by applying a filtering operator to the Navier-Stokes equations, the LES equations are obtained, which can be written as follows:

$$\frac{\partial \langle W \rangle + W^c}{\partial t} + \nabla \cdot F(\langle W \rangle + W^c) = -\tau^{LES}(\langle W \rangle + W^c) \tag{6}$$

where τ^{LES} is the SGS term.

An equation for the resolved fluctuations W^c can thus be derived (see also [12]):

$$\frac{\partial W^c}{\partial t} + \nabla \cdot F(\langle W \rangle + W^c) \; - \; \nabla \cdot F(\langle W \rangle) = \tau^{RANS}(\langle W \rangle) - \tau^{LES}(\langle W \rangle + W^c) \tag{7}$$

The basic idea of the proposed hybrid model is to solve Eq.(5) in the whole domain and to correct the obtained averaged flow by adding the remaining resolved fluctuations (computed through Eq.(7)), wherever the grid resolution is adequate for a LES. To identify the regions where the additional fluctuations must be computed, we introduce a *blending function*, θ, smoothly varying between 0 and 1. When $\theta = 1$, no correction to $\langle W \rangle$ is computed and, thus, the RANS approach is recovered. Conversely, wherever $\theta < 1$, additional resolved fluctuations are computed; in the limit of $\theta \to 0$ we want to recover a full LES approach. Thus, the following equation is used here for the correction term:

$$\begin{array}{l} \dfrac{\partial W^c}{\partial t} \; + \; \nabla \cdot F(\langle W \rangle + W^c) \; - \; \nabla \cdot F(\langle W \rangle) = \\ (1-\theta) \left[\tau^{RANS}(\langle W \rangle) - \tau^{LES}(\langle W \rangle + W^c) \right] \end{array} \tag{8}$$

Although it could seem rather arbitrary from a physical point of view, in Eq.(8) the damping of the right hand side term through multiplication by $(1-\theta)$ is aimed to obtain a smooth transition between RANS and LES. More specifically, we wish to obtain a progressive addition of fluctuations when the grid resolution increases and the model switches from the RANS to the LES mode.

Summarizing, the ingredients of the proposed approach are: a RANS closure model, a SGS model for LES and the definition of the blending function.

2.2.1 RANS and LES closures:

For the LES mode, we wish to recover the variational multiscale approach described in Section 2.1. Thus, the Galerkin projection of the equations for averaged flow and for correction terms in the proposed hybrid model become respectively:

$$\begin{array}{l}\left(\dfrac{\partial\langle W\rangle}{\partial t},\psi_l\right)+(\nabla\cdot F_c(\langle W\rangle),\psi_l)+(\nabla\cdot F_v(\langle W\rangle),\phi_l)= \\ -\left(\tau^{RANS}(\langle W\rangle),\phi_l\right)\quad l=1,N\end{array} \tag{9}$$

$$\begin{array}{l}\left(\dfrac{\partial W^c}{\partial t},\psi_l\right)+(\nabla\cdot F_c(\langle W\rangle+W^c),\psi_l)-(\nabla\cdot F_c(\langle W\rangle),\psi_l)+ \\ (\nabla\cdot F_v(W^c),\phi_l)=(1-\theta)\left[\left(\tau^{RANS}(\langle W\rangle),\phi_l\right)-\left(\tau^{LES}(W'),\phi_l'\right)\right]\quad l=1,N\end{array} \tag{10}$$

where $\tau^{RANS}(\langle W\rangle$ is the closure term given by a RANS turbulence model and $\tau^{LES}(W')$ is given by one of the SGS closures mentioned in Section 2.1.

As far the closure of the RANS equations is concerned, the low Reynolds $k-\varepsilon$ model proposed in [4] is used.

2.2.2 Definition of the blending function and simplified model:

As a possible choice for θ, the following function is used in the present study:

$$\theta=F(\xi)=tanh(\xi^2) \tag{11}$$

where ξ is the *blending parameter*, which should indicate whether the grid resolution is fine enough to resolve a significant part of the turbulence fluctuations, i.e. to obtain a LES-like simulation. The choice of the *blending parameter* is clearly a key point for the definition of the present hybrid model. In the present study, different options are proposed and investigated, namely: the ratio between the eddy viscosities given by the LES and the RANS closures and the ratio between the LES filter width and a typical length in the RANS approach.

To avoid the solution of two different systems of PDEs and the consequent increase of required computational resources, Eqs. (9) and (10) can be recast together as:

$$\begin{array}{l}\left(\dfrac{\partial W}{\partial t},\psi_l\right)+(\nabla\cdot F_c(W),\psi_l)+(\nabla\cdot F_v(W),\phi_l)= \\ -\theta\left(\tau^{RANS}(\langle W\rangle),\phi_l\right)-(1-\theta)\left(\tau^{LES}(W'),\phi_l'\right)\quad l=1,N\end{array} \tag{12}$$

Clearly, if only Eq. (12) is solved, $\langle W\rangle$ is not available at each time step. Two different options are possible: either to use an approximation of $\langle W\rangle$ obtained by averaging and smoothing of W, in the spirit of VMS, or to simply use in Eq. (12) $\tau^{RANS}(W)$. The second option is adopted here as a first approximation. We refer to [20, 18] for further details.

3 Numerical method and parallelisation strategy

The fluid solver AERO under consideration is based on a mixed finite element/finite volume formulation on unstructured tetrahedral meshes. The scheme is vertex-centered, the diffusive terms are discretized using P1 Galerkin finite elements and the convective terms with finite volumes. The Monotone Upwind Scheme for Conservation Laws reconstruction method (MUSCL) is adopted here

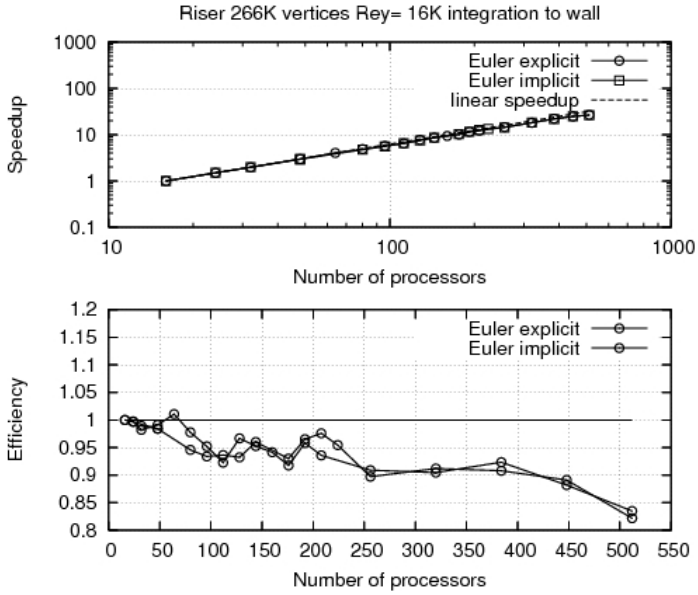

Figure 1: Speedup and efficiency on SGI ICE 8200EX for a 266K vertices geometry, measured on the calculation of explicit and implicit Euler flow, from 16 cores to 512.

and the scheme is stabilized with sixth-order spatial derivatives. An upwind parameter γ, which multiplies the stabilization part of the scheme, allows a direct control of the numerical viscosity, leading to a full upwind scheme for $\gamma = 1$ and to a centered scheme for $\gamma = 0$. This low-diffusion MUSCL reconstruction, which limits as far as possible the interaction between numerical and SGS dissipation, is described in detail in [2] and [15].

The flow equations are advanced in time with an implicit scheme, based on a second-order time-accurate backward difference scheme. The non-linear discretised equations are solved by a defect-correction (Newton-like) method in which a first order semi-discretisation of the Jacobian is used. At each time-step, the resulting sparse linear system is solved by a Restricted Additive Schwarz (RAS) method [21]. More specifically, the linear solver is based on GMRES with a RAS preconditioning and the subdomain problems are solved with ILU(0). Typically, two defect-correction iterations requiring each of them a maximum of 20 RAS iterations are used per time-step. This implicit scheme is linearly unconditionally stable and second-order accurate.

For what concerns the parallelisation strategy used in this study, it combines mesh partitioning techniques and a message-passing programming model [9, 13]. The mesh is assumed to be partitioned into several submeshes, each one defining a subdomain. Basically the same serial code is going to be executed within every subdomain. Modifications for parallel implementation occured in the main stepping-loop in order to take into account several assembly phases of the subdomain results, depending on the fluid equations (viscous/inviscid flows), the spatial approximation and on the nature of the time advancing procedure (explcit/implicit). Because mesh partitions with overlapping incur redundant floating-point operations, non-overlapping mesh partitions are chosen. It has been shown in [13] that the latter option is more efficient though it induces additional

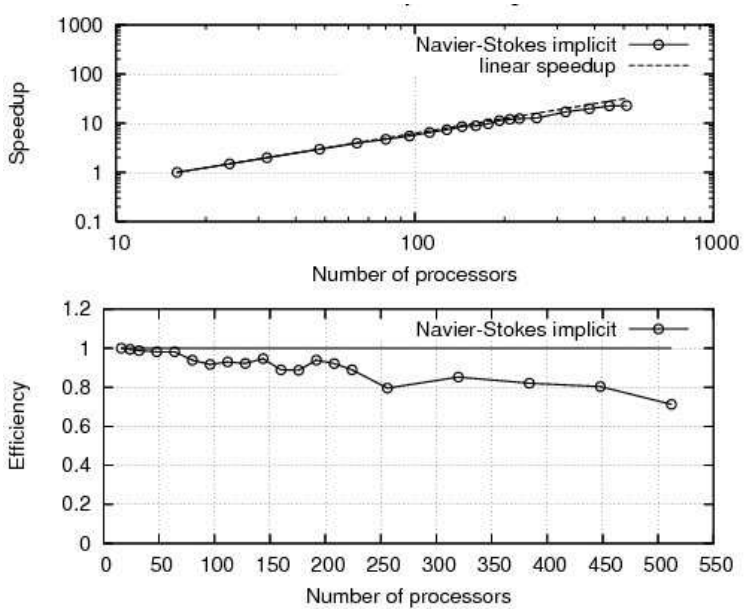

Figure 2: Speedup and efficiency on SGI ICE 8200EX for a 266K vertices geometry: speedup from 16 cores to 512, measures on the calculation of implicit Navier-stokes flow.

communication steps. For our applications, in a preprocessing step we use an automatic mesh partitioner that creates load balanced submeshes inducing a minimum amount of interprocessor communications. Data communications between neighboring subdomains are achieved through the MPI communication library.

We present a few speedup performances measured on three different computing configurations:
- Configuration 1 is a SGI ICE 8200EX with 3GHz Xeon processors ("jade", Figs.1-2).
- Configuration 2 is a homogeneous cluster from the Sophia Antipolis Grid 5000 site (Fig.4).
- Configuration 3 is a heterogeneous cluster from the Sophia Antipolis Grid 5000 site (Fig.5).

The sequences to be computed are:
- 200 explicit time steps, for Euler model or for the Navier-Stokes model using the VMS-LES turbulence model.
- 200 implicit time steps, involving for each 40 RAS-GMRES sweeps, for Euler model or for the complete Navier-Stokes model.

A typical time for the explicit Euler test is for 32 processors 678 seconds on SGI ICE 8200EX and 1077 seconds on Grid 5000 (ratio is 1.56).

A first comment is the strong impact on communication speed on speedup. Indeed we verify that the newer architecture ICE 8200EX still shows a good speedup with 512 processors/cores although a rather small amount of computation is made in each processor since the number of mesh vertices per processor is about 5000.

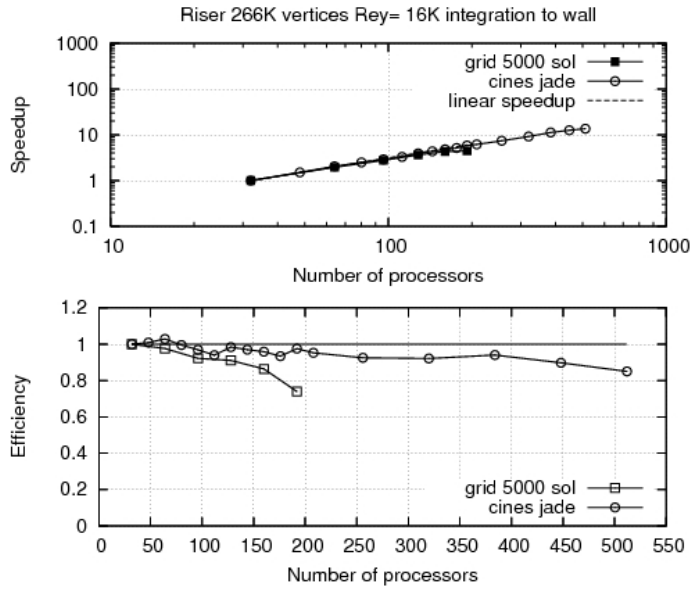

Figure 3: Speedup and efficiency on SGI ICE 8200EX and G5000 homogeneous cluster for a 266K vertices geometry: speedup from 16 cores to 512, measures on the calculation of explicit Euler flow.

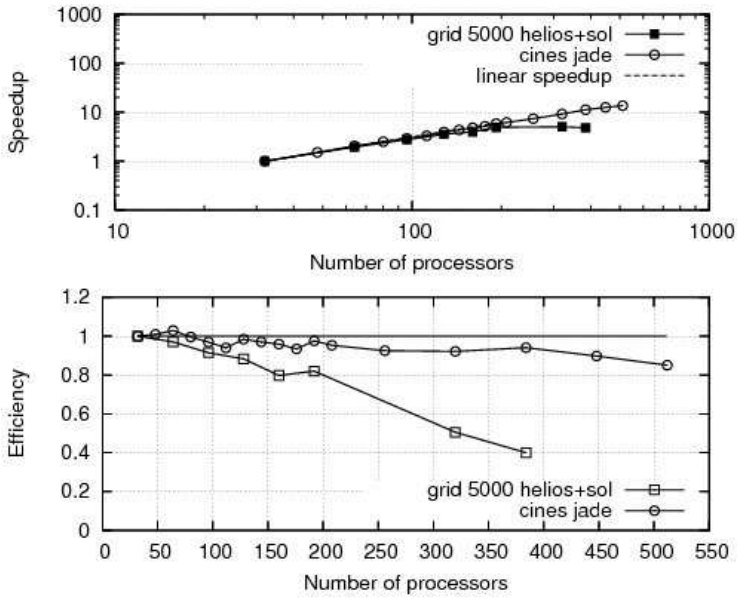

Figure 4: Speedup and efficiency on SGI ICE 8200EX and G5000 heterogeneous cluster for a 266K vertices geometry: speedup from 16 cores to 512, measures on the calculation of explicit Euler flow.

A second comment is that the complexity of the Navier-Stokes LES model have some consequence on the speedup.

For the simulations presented in the next section, the Roe-Turkel solver is used with a numerical viscosity parameter γ belonging to the interval $[0.2, 0.3]$. The CFL number was chosen so that a vortex shedding cycle is sampled in around 400 time steps for the low-Reynolds simulations and at least 1500 time steps for the simulations at Re =140000.

4 VMS-LES Simulations

In this section, we apply our VMS-LES methodology to the simulation of a flow past a circular cylinder at Mach number $M_\infty = 0.1$ and at a subcritical Reynolds number, based on body diameter and freestream velocity, equal to 3900.

The computational domain size is: $-10 \leq x/D \leq 25$, $-20 \leq y/D \leq 20$ and $-\pi/2 \leq z/D \leq \pi/2$, where x, y and z denote the streamwise, transverse and spanwise direction respectively. The cylinder of unit diameter D is centered on $(x, y) = (0, 0)$.

For the purpose of these simulations, the Steger-Warming conditions [25] are imposed at the inflow and outflow as well as on the upper and lower surface
($y = \pm H_y$). In the spanwise direction periodic boundary conditions are applied and on the cylinder surface no-slip boundary conditions are set.

The flow domain is discretized by two unstructured tetrahedral grids: the first one (GR1) consists of approximately 2.9×10^5 nodes. The averaged distance of the nearest point to the cylinder boundary is $0.017D$, which corresponds to $y^+ \approx 3.31$. The second grid (GR2) is obtained from GR1 by refining in a *structured* way, i.e. by dividing each tetrahedron in 4, resulting in approximately 1.46×10^6 nodes. A large number of simulations were carried out by varying different parameters, as, for instance, the SGS model, the value of γ_s or the grid resolution. We report here only the results obtained in some of these simulations. The main parameters of the considered simulations are summarized in Tab.1, together with some of the obtained flow bulk parameters. The experimental reference value for the mean drag coefficient, $\overline{C_d}$, is 0.99 ± 0.05 from [17], which well agrees with those computed in well resolved LES in the literature [11, 7], while for the vortex-shedding Strouhal number, St, values in the range of $[0.21, 0.22]$ are generally obtained. Finally, for the mean recirculation bubble length, a recent experimental and numerical study [19] seems to indicate a reference value of $l_r = 1.51 \pm 10\%$. Fig.5a shows the mean pressure coefficient distribution at the cylinder obtained on GR1 in LES and VMS-LES simulations, together with experimental data from [17]. From the discrepancy between numerical results and experimental data in the zone of the negative peak it is evident that in all cases the boundary layer evolution is not accurately captured in the simulations, due to the grid coarseness. Another symptom of a too coarse grid resolution (see the discussion in [11]) is the underestimation of the mean recirculation length l_r in all the simulations on GR1 (Tab.1). However, some differences exist between the LES and the VMS-LES simulations. In particular, in LES the discrepancy observed in the negative peak of mean C_p is larger and the differences among the different SGS models are more pronounced than in VMS-LES. This is due to the fact that the non-dynamic eddy-viscosity models here used, although mainly acting in the wake, also provide a significant SGS viscosity in the laminar regions, as the boundary layer and the detaching shear layers (see, e.g., Fig.6a). In the VMS-LES simulations the spatial distribution of the SGS viscosity is qualitatively similar to that obtained in LES, but the amount is significantly reduced everywhere (compare the scales of Fig.6a and Fig.6b), and, thus, also in the laminar zones. Moreover, we recall that in the VMS-LES approach the SGS viscosity

Table 1: Main simulation parameters and flow bulk coefficients.

Turb. model	SGS model	Grid	γ_s	$\overline{C_d}$	St	l_r
LES	Smagorinsky	GR1	0.3	1.16	0.212	0.81
LES	Vreman	GR1	0.3	1.04	0.221	0.97
LES	WALE	GR1	0.3	1.14	0.214	0.75
VMS-LES	Smagorinsky	GR1	0.3	1.00	0.221	1.05
VMS-LES	Vreman	GR1	0.3	1.00	0.22	1.07
VMS-LES	WALE	GR1	0.3	1.03	0.219	0.94
no model	-	GR1	0.3	0.96	0.223	1.24
no model	-	GR1	0.2	0.94	0.224	1.25
LES	WALE	GR2	0.3	1.02	0.221	1.22
VMS-LES	WALE	GR2	0.3	0.94	0.223	1.56
no model	–	GR2	0.3	0.92	0.225	1.85

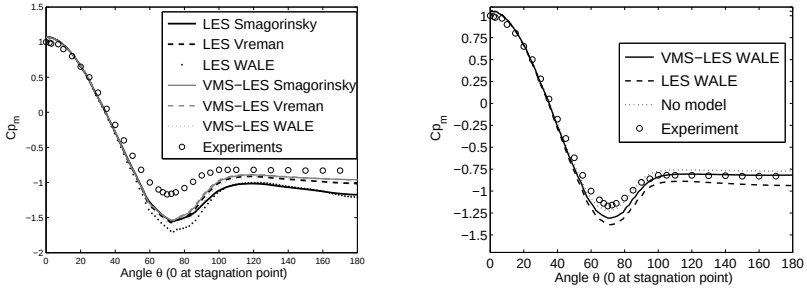

(a) (b)

Figure 5: Mean pressure coefficient distribution at the cylinder. (a) Simulations on GR1, (b) Simulations on GR2.

only acts on the smallest resolved scales. The different distribution of SGS viscosity leads in LES to additional inaccuracies, besides those due to grid coarseness and previously discussed, which are not present in VMS-LES. For instance, Fig.5a shows that the base pressure is inaccurately predicted in all LES simulations except for the Vreman model, leading to an inaccurate value of the mean drag coefficient (Tab.1) while for the VMS-LES ones the agreement with the experiments is fairly good. The pressure distribution obtained in the simulations without any SGS model (not shown) is very similar to the one obtained in the VMS-LES ones, as well as for low-order velocity statistics in the wake and for the bulk flow parameters, except than for a significantly higher l_r given by the no-model simulations (Tab.1). This is an a-posteriori confirmation that the used MUSCL reconstruction indeed introduces a viscosity acting only on the highest resolved frequencies [2], as the SGS viscosity in the VMS approach and that this limits its negative effects. Moreover, the results obtained with two different(low) values of the parameter γ_s are also very similar (Tab.1), consistently with our previous findings [2]. As for the results on the refined grid GR2, as expected, in both LES and VMS-LES the agreement with the reference data is improved. However, in LES discrepancies are still observed (see, e.g., Fig.5b) due to the excessive introduced SGS viscosity, while with VMS-LES a general good agreement is obtained. Note that in this case, although for

the pressure distribution, and thus for the drag coefficient, the simulation without any model gives accurate results, the length of the mean recirculation bubble is largely overestimated, due indeed to the lack of SGS viscosity in the wake.

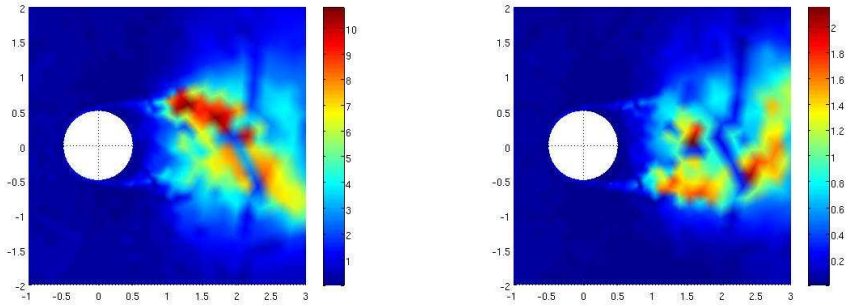

(a) (b)

Figure 6: Instantaneous iso-contours of μ_s/μ. Simulations on GR1 with the Smagorinsky SGS model: (a) LES, (b) VMS-LES.

The Fourier energy spectrum of the spanwise velocity at P(3, 0.5, 0) for Vreman SGS model with LES and VMS-LES on the coarse grid GR1 is displayed in Fig.7. The frequency is nondimensionalized by the Strouhal shedding frequency. Via the Taylor hypothesis of frozen turbulence (which is justified since the mean convection velocity is large at that point) which allows to assume that high (low) time frequencies correspond to small (large) scale in space, we observe that the energy in the large resolved scales are higher with VMS-LES than with LES. These results corroborate the fact that in the VMS-LES approach, the modeling of the energy dissipation effects of the unresolved scales affects only the small resolved scales, unlikely in the LES approach in which these dissipative effects act on all the resolved scales.

Summarizing, our results confirm that the idea of concentrating the SGS viscosity only on the smallest resolved scales actually permits to use simple eddy-viscosity SGS models and to obtain

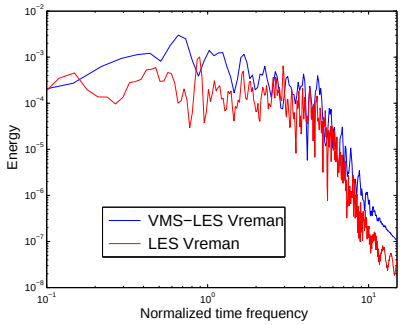

Figure 7: Fourier energy spectrum: spanwise velocity for LES Vreman and VMS-LES Vreman

accurate results, comparable to those obtained in the literature with dynamic models. We recall that on unstructured grids this leads to significantly more affordable simulations, since the cost of the dynamic procedure may become prohibitive. In the same spirit, it has been confirmed that the fact of also concentrating the numerical dissipation on the smallest resolved scales permits to limit its negative effects.

For this problem involving 1.5 million degrees of freedom and for twenty shedding cycles simulation, the simulation time is about 7 hours on a 32-processor IBM Power 4 computer.

5 Hybrid RANS/VMS-LES Simulations

The new proposed hybrid model (*Fluctuation Correction Model*, FCM) has been applied to the simulation of the flow around a circular cylinder at $Re = 140000$ (based on the far-field velocity and the cylinder diameter). The domain dimensions are: $-5 \leq x/D \leq 15$, $-7 \leq y/D \leq 7$ and $0 \leq z/D \leq 2$ (the symbols are the same as in Section 4). Two grids have been used, the first one (GR1) has 4.6×10^5 nodes, while the second one has (GR2) 1.4×10^6 nodes. Both grids are composed of a structured part around the cylinder boundary and a unstructured part in the rest of the domain. The inflow conditions are the same as in the DES simulations of Travin et al. [26]. In particular, the flow is assumed to be highly turbulent by setting the inflow value of eddy-viscosity to about 5 times the molecular viscosity as in the DES simulation of Travin et al. [26]. This setting corresponds to a free-stream turbulence level $\overline{u'^2}/U_0$ (where u' is the inlet velocity fluctuation and U_0 is the free-stream mean velocity) of the order of 4%. As discussed also by Travin et al. [26], the effect of such a high level of free-stream turbulence is to make the boundary layer almost entirely turbulent also at the relatively moderate considered Reynolds number. The boundary treatment is the same as for the VMS-LES simulations in Section 4, except that wall laws are now used. The RANS model is that based on the low-Reynolds approach [4]. The LES closure is based on the VMS approach (see Section2.1). The SGS models used in the simulations are those given in Section2. The main parameters characterizing the simulations carried out with the FCM are summarized in Tab.2. The main flow bulk parameters obtained in the present simulations are summarized in

Simulation	Blending parameter	Grid	LES-SGS model
FCM1	VR	GR1	Smagorinsky
FCM2	LR	GR1	Smagorinsky
FCM3	LR	GR2	Smagorinsky
FCM4	LR	GR1	Vreman
FCM5	LR	GR1	Wale

Table 2: Simulation name and their main characteristics

Tab.3, together with the results of DES simulations in the literature and some experimental data. They have been computed by averaging in time, over at least 20 shedding cycles and in the spanwise direction. Let us analyze, first, the sensitivity to the blending parameter, by comparing the results of the simulation FCM1 and FCM2. The results are practically insensitive to the definition of the blending parameter. Conversely, the grid refinement produces a delay in the boundary layer separation which results in a decrease of $\bar{C}_d$ (compare FCM2 and FCM3). However, note that, for unstructured grids, the refinement changes the local quality of the grid (in terms of homogeneity and regularity of the elements) and this may enhance the sensitivity of the results. The sensitivity to the VMS-LES closure model is also very low (compare FCM2, FCM4 and FCM5). This very low

Data from	Re	$\overline{C_d}$	C_l'	St	l_r	θ_{sep}
FCM1	**1.4 10^5**	**0.62**	**0.083**	**0.30**	**1.20**	**108**
FCM2	**1.4 10^5**	**0.62**	**0.083**	**0.30**	**1.19**	**108**
FCM3	**1.4 10^5**	**0.54**	**0.065**	**0.33**	**1.13**	**115**
FCM4	**1.4 10^5**	**0.65**	**0.077**	**0.28**	**1.14**	**109 (99)**
FCM5	**1.4 10^5**	**0.66**	**0.094**	**0.28**	**1.24**	**109 (100)**
Numerical data						
DES [26]	1.4 10^5	0.57-0.65	0.08-0.1	0.28-0.31	1.1 -1.4	93-99
DES [14]	1.4 10^5	0.6-0.81	–	0.29-0.3	0.6-0.81	101-105
Experiments						
[8]	3.8 10^6	0.58	–	0.25	–	110
[1]	5 10^6	0.7	–	–	–	112
[22]	8 10^6	0.52	0.06	0.28	–	–

Table 3: Main bulk flow quantities for the circular cylinder test case. Same notations as in Tab.??.

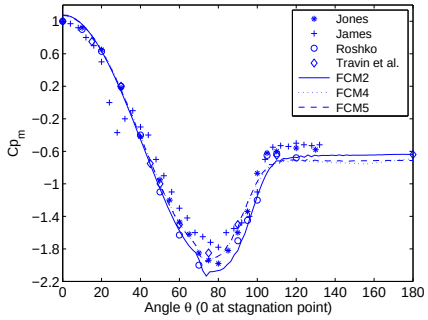

Figure 8: $\bar{C}_p$ on the cylinder surface compared to numerical and experimental results

sensitivity has been observed also in VMS-LES simulations at low Reynolds number see Section4 and, thus, it seems more peculiar to the VMS-LES approach rather than to the hybrid model. The agreement with the DES results is fairly good. As for the comparison with the experiments, as also stated in Travin et al. [26], since our simulations are characterized by a high level of turbulence intensity at the inflow, it makes sense to compare the results with experiments at higher Reynolds number, in which, although the level of turbulence intensity of the incoming flow is very low, the transition to turbulence of the boundary layer occurs upstream separation. The agreement with these high Re experiments is indeed fairly good, as shown in Tab.3 and in Fig.8. The behavior of the separation angle requires a brief discussion. There is a significant discrepancy between the values obtained in DES and the experimental ones. For our simulations, the values of θ_{sep} shown in Tab.3 are estimated by considering the point at which the C_p distribution over the cylinder becomes nearly constant (see e.g. Fig.8), as usually done in experimental studies. Indeed, the reported values are generally in better agreement with the experiments than those obtained by DES. However, if we estimate the separation angle from the streamlines of the average or instantaneous velocity fields, significantly lower values are found (reported in parentheses in Tab.3 for the simulations FCM4 and FCM5); these values are closer to those obtained by DES. Finally, the model works in RANS mode in the boundary layer and in the shear-layers detaching from the cylinder, while in the wake a full

VMS-LES correction is recovered.
For this problem involving 3.2 million degrees of freedom and for twenty shedding cycles simulation, the simulation time is about 30 hours on a 32-processor IBM Power 4 computer and about 16 hours on a 32-processor IBM Power 5 computer.

6 Conclusion

In this paper we have presented parallel simulations of three-dimensional turbulent flows. An efficient implicit time advancing can be applied with a rather small time step and small computational effort. In these conditions, a good speedup for 16-512 cores is obtained with a recent parallel architecture. With this tool, we have first investigated the application of a Variational multiscale LES for the simulations of a flow past a circular cylinder at a subcritical Reynolds number equal to Re =3900. Although a rather coarse grid has been used, this model gives accurate predictions of bulk coefficients and shows that two recently developed SGS models, the Vreman's model and the WALE model combine well in the VMS formulation. Moreover, it appears in this approach that the influence of the SGS model is weak, but this seems to give a support to the VMS idea of adding some dissipation only to the smallest resolved scales. In a second part, we have presented a hybrid RANS/LES approach using different definitions of blending parameter and SGS models. For the closure of the LES part, the VMS approach has been used. This model is validated on the prediction of a flow around a circular cylinder at higher Reynolds number (Re =140000). The results obtained correlate well with the experimental and numerical data from the literature as well as the behavior of the blending function.

7 Acknowledgements

We thank Eric lamballais for kindly providing experimental data concerning the Re=3900 test case.

Some experiments presented in this paper were carried out using the Grid'5000 experimental testbed, being developed under the INRIA ALADDIN development action with support from CNRS, RENATER and several Universities as well as other funding bodies (see https://www.grid5000.fr).

The authors would like also to acknowledge the support of Centre Informatique National de l'Enseignement Supérieur (CINES[1]), Montpellier, FRANCE, and the support of PACA[2] region for the cooperation between INRIA and the University of Montpellier. The CINES results were made on the SGI ICE 8200EX parallel machine.

CINECA (Bologna, Italy), IDRIS (Orsay, France) and INRIA-Sophia Cluster are also gratefully acknowledged for having provided computational resources for this study.

References

[1] E. Achenbach. Distribution of local pressure and skin friction around a circular cylinder in cross-flow up to Re= 5×10^6. *J. Fluid Mech.*, 34(4):625–639, 1968.

[1] http://www.cines.fr
[2] Provence-Alpes-Côte-d'Azur

[2] S. Camarri, M.V. Salvetti, B. Koobus, and A. Dervieux. A low diffusion MUSCL scheme for LES on unstructured grids. *Computers and Fluids*, 33:1101–1129, 2004.

[3] S.S. Collis and Y. Chang. The DG/VMS method for unified turbulence simulation. AIAA paper 2002-3124, 2002.

[4] U. Goldberg, O. Peroomian, and S. Chakravarthy. A wall-distance-free $k-\varepsilon$ model with enhanced near-wall treatment. *Journal of Fluids Engineering*, 120:457–462, 1998.

[5] T.J.R. Hughes, L. Mazzei, and K.E. Jansen. Large eddy simulation and the variational multiscale method. *Comput. Vis. Sci.*, 3:47–59, 2000.

[6] T.J.R. Hughes, A.A. Oberai, and L. Mazzei. Large eddy simulation of turbulent channel flows by the variational multiscale method. *Phys Fluids*, 13:1784–1799, 2001.

[7] S. Lee J. Lee N. Park and H. Choi. A dynamical subgrid-scale eddy viscosity model with a global model coefficient. *Physics of Fluids*, 2006.

[8] W.D. James, S.W. Paris, and G.V. Malcolm. Study of viscous cross flow effects on circular cylinders at high Reynolds numbers. *AIAA Journal*, 18:1066–1072, 1980.

[9] B. Koobus, S. Camarri, M.V. Salvetti, S. Wornom, and A. Dervieux. Parallel simulation of three-dimensional complex flows: Application to turbulent wakes and two-phase compressible flows. *Advances in Engineering Software*, 38:328–337, 2007.

[10] B. Koobus and C. Farhat. A variational multiscale method for the large eddy simulation of compressible turbulent flows on unstructured meshes-application to vortex shedding. *Comput. Methods Appl. Mech. Eng.*, 193:1367–1383, 2004.

[11] A.G. Kravchenko and P. Moin. Numerical studies of flow over a circular cylinder at $re_d = 3900$. *Physics of fluids*, 12:403–417, 1999.

[12] E. Labourasse and P. Sagaut. Reconstruction of turbulent fluctuations using a hybrid RANS/LES approach. *J. Comp. Phys.*, 182:301–336, 2002.

[13] S. Lanteri. Parallel solutions of three-dimensional compressible flows. Technical Report RR-2594, INRIA, 1995.

[14] S.-C. Lo, K.A. Hofmann, and J.-F. Dietiker. Numerical investigation of high Reynolds number flows over square and circular cylinder. *Journal of Thermophysics and Heat Transfer*, 19:72–80, 2005.

[15] V. Mariotti, S. Camarri, M.-V. Salvetti, B. Koobus, A. Dervieux, H. Guillard, and S. Wornom. Numerical simulation of a jet in crossflow. Application to GRID computing. Technical Report RR-5638, 2005.

[16] F. Nicoud and F. Ducros. Subgrid-scale stress modelling based on the square of the velocity gradient tensor. *Flow, Turbulence and Combustion*, 62:183–200, 1999.

[17] C. Norberg. Effects of Reynolds number and low-intensity free-sream turbulence on the flow around a circular cylinder. *Publ. No. 87/2, Department of Applied Termosc. and Fluid Mech.*, 1987.

[18] G. Pagano, S. Camarri, M.V. Salvetti, B. Koobus, and A. Dervieux. Strategies for RANS/VMS-LES coupling. Technical Report RR-5954, INRIA, 2006.

[19] P. Parneaudeau, J. Carlier, D. Heitz, and E. Lamballais. Experimental and numerical studies of the flow over a circular cylinder at Reynolds number 3900. *Phys. Fluids*, 20(085101), 2008.

[20] M.V. Salvetti, B. Koobus, S. Camarri, and A. Dervieux. Simulation of bluff-body flows through a hybrid RANS/VMS-LES model. In *Proceedings of the IUTAM Symposium on Unsteady Separated Flows and their Control*, Corfu (Grece), June 18-22 2007.

[21] M. Sarkis and B. Koobus. A scaled and minimum overlap restricted additive schwarz method with application on aerodynamics. *Comput. Methods Appl. Mech. Eng.*, 184:391–400, 2000.

[22] J.W. Schewe. On the forces acting on a circular cylinder in cross flow from subcritical up to transcritical Reynolds numbers. *J. Fluid Mech.*, 133:265–285, 1983.

[23] J. Smagorinsky. General circulation experiments with the primitive equations. *Monthly Weather Review*, 91(3):99–164, 1963.

[24] P.R. Spalart, W.H. Jou, M. Strelets, and S. Allmaras. *Advances in* DNS/LES, chapter Comments on the feasibility of LES for wings and on a hybrid RANS/LES approach. Columbus (OH), 1997.

[25] J.L. Steger and R.F. Warming. Flux vector splitting for the inviscid gas dynamic equations with applications to the finite difference methods. *J. Comp. Phys*, 40(2):263–293, 1981.

[26] A. Travin, M. Shur, M. Strelets, and P. Spalart. Detached-eddy simulations past a circular cylinder. *Flow, Turbulence and Combustion*, 63:293–313, 1999.

[27] A.W. Vreman. An eddy-viscosity subgrid-scale model for turbulent shear flow: algebraic theory and application. *Physics of Fluids*, 16:3670–3681, 2004.

Unité de recherche INRIA Sophia Antipolis
2004, route des Lucioles - BP 93 - 06902 Sophia Antipolis Cedex (France)

Unité de recherche INRIA Futurs : Parc Club Orsay Université - ZAC des Vignes
4, rue Jacques Monod - 91893 ORSAY Cedex (France)
Unité de recherche INRIA Lorraine : LORIA, Technopôle de Nancy-Brabois - Campus scientifique
615, rue du Jardin Botanique - BP 101 - 54602 Villers-lès-Nancy Cedex (France)
Unité de recherche INRIA Rennes : IRISA, Campus universitaire de Beaulieu - 35042 Rennes Cedex (France)
Unité de recherche INRIA Rhône-Alpes : 655, avenue de l'Europe - 38334 Montbonnot Saint-Ismier (France)
Unité de recherche INRIA Rocquencourt : Domaine de Voluceau - Rocquencourt - BP 105 - 78153 Le Chesnay Cedex (France)

Éditeur
INRIA - Domaine de Voluceau - Rocquencourt, BP 105 - 78153 Le Chesnay Cedex (France)
http://www.inria.fr
ISSN 0249-6399